Arch. Metall. Mater. **64** (2019), 3, 819-822

DOI: 10.24425/amm.2019.129454

HEONSEOP SHIN*†, DOYEON HAN*†, SANGHOON KIM*#, SUNGSOO RHIM*

CALIBRATION OF VISCO-HYPERELASTIC MODEL FOR TENSILE BEHAVIOR OF PORCINE SKIN

Uniaxial tensile tests were performed on porcine skin to investigate the tensile stress-strain constitutive characteristic at quasistatic deformations using uniaxial tensile tests. Experimental results were then used to determine the parameters of the various constitutive model types for rubber, including the Mooney-Rivlin, Yeoh, Ogden, and others. The Prony series viscoelastic model was also calibrated based on the stress relaxation test. To investigate the calibrated constitutive equations (visco-hyperelastic), the falling impact test was conducted. From the viewpoint of the maximum impact load, the error was approximately 15.87%. Overall, the Ogden model predicted the experimental measurements most reasonably. The calibrated constitutive model is expected to be of practical use in describing the mechanical properties of porcine skin.

Keywords: Porcine skin, Skin layers, Visco-hyperelastic, Constitutive model

1. Introduction

In the era of collaborative environments between industrial robots and humans, the problem of collision safety has become increasingly important for the robot market. In order to implement collaborative operations, it is necessary to prevent the dynamic motion of the robot from harming people. To properly estimate the damage, it is essential to use the modeling and simulation (M&S) method of human-robot collision to evaluate the robot motion that would be imposed on the human body [1-4]. In order to analyze the responses of human beings, it is important to study and analyze their skin properties.

Skin is a complex multilayer material consisting mainly of the epidermis, dermis, and hypodermis. In many applications, not only the quasistatic, but also the viscoelastic behavior of skin is important [5-8]. Therefore, there have been a number of studies on the formulation and characterization of the constitutive model of the mechanical properties of various skins types in vivo, such as the human, rat, pig, and others [9-14].

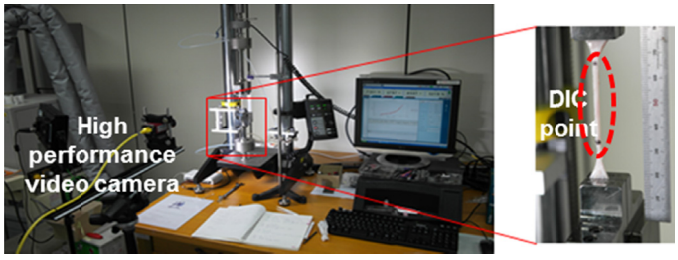

Fig. 1. Setup for the uniaxial tensile stress relaxation test

In this study, we calibrated the constitutive equation of pig skin based on quasistatic nonlinear elasticity and viscoelasticity. Among all the skin types studied, porcine skin was chosen because of its close resemblance and mechanical response to human skin. Additionally, impact tests were conducted to verify the visco-hyperelastic model of porcine skin.

2. Experimental

2.1. Tensile test

An INSTRON 5848 testing machine was used to conduct the quasistatic tensile tests. Tensile loads and displacements were measured directly by a load cell and a video camera system. According to a previous study [15], the quasistatic cyclic tensile test was performed on skin specimens at a constant strain rate of 10^{-3}/s. The test animals were white Yucatan minipigs, 100 days old, with a weight of approximately 10 kg. The detailed descriptions for the tensile tests are submitted in Archives of Metallurgy and Materials.

2.2. Stress relaxation test

As it can be observed in Fig. 1, tensile load was applied to the specimen at a speed of 500 mm/min using INSTRON 5848 as part of the tensile stress relaxation test. The specimen was stretched using a strain of approximately 20%, and the load was

* DEPARTMENT OF MECHANICAL ENGINEERING, KYUNG HEE UNIVERSITY, 1732 DEOKYOUNGDAERO, GIHEUNG-GU, YONGIN-SI, GYEONGGI 17104, KOREA

Corresponding author: kimsh83@khu.ac.kr

† These authors are co-first authors

then measured [16]. The shape of the specimen was the same as that of the specimen used in the tensile test. In this experiment, the strain of the specimen was measured using a video camera in the form of a noncontact extensometer.

2.3. Free falling impact test and development of finite element model

The free-falling impact test in Fig. 2(a) was conducted in order to simulate the situation where an impact occurs between the human and the manipulator. Additionally, we can validate the visco-hyperelastic model of porcine skin by conducting this test. The specimen is constraint-free, and the experiment was performed by the free falling of the impactor with a load of 9.5 kg. The mass of the impactor was determined by referring to the payload and the effective mass of the robot motion. By controlling the height of the impactor, we also controlled the velocity of the impactor to a value of 0.5 m/s. The dimensions of the skin samples were 80 mm × 40 mm × 5 mm. Additionally, the shape of impactor was based on a wedge shape (radius = 5 mm).

As it can be observed in Fig. 2(b), the finite element method (FEM) model was developed by replicating the free fall experimental environment. In this instance, it was developed as a 1/2 symmetric model to shorten the analysis time. For the physical properties of porcine skin, we input the visco-hyperelastic parameters based on the calibrated quasistatic/stress relaxation tensile tests. The constraint and the load condition were implemented in the same way as the conditions in the free-falling test. A commercial pre/postprocessor (ABAQUS CAE) was used in this process.

3. Results and discussion

As it can be observed in Fig. 3(a) and (b), a uniaxial tensile test at a quasistatic condition was conducted to calibrate parameters of the hyperelastic constitutive equations. In this study, we used the tools provided by ABAQUS CAE to determine the optimal fitting values of the experimental data [17]. Table 1 shows the calibrated Ogden model parameters. Although the Yeoh and Mooney-Rivlin models are associated with low-fitting errors, these models are not stable for all strains. Thus, these two models cannot be used as the constitutive models in ABAQUS CAE. Therefore, the Ogden model in Eq. (1) was used to evaluate the capability of the hyperelastic constitutive equation to describe the mechanical behavior of porcine skin with each of the skin specimens used in this study.

TABLE 1

Calibrated parameters of the Ogden model for the porcine skin layer

I (region)	μ_I (MPa)	α_I	D_I
1 (dermis)	1.077	20.780	3.736E-02
1 (hypodermis)	2.322	8.107	1.733E-02

$$W = \sum_{i=1}^{N} \frac{2\mu_i}{\alpha_i^2}\left(\overline{\lambda_1}^{\alpha_i} + \overline{\lambda_2}^{\alpha_i} + \overline{\lambda_3}^{\alpha_i} - 3\right) + \sum_{i=1}^{N} \frac{1}{D_i}\left(J_{el} - 1\right)^{2i} \quad (1)$$

where $\overline{\lambda_i}$ is the deviatoric principal stretch, and μ_i and α_i are temperature-dependent material constants. It is known that the model captures the upturn stress-strain curve and accurately describes the behavior of rubber in a wide range of deformation.

Stress relaxation is a phenomenon in which the stress of a specimen is continuously reduced when the specimen is held in a stretched or compressed state with a certain length. In this case, time-dependent mechanical properties are derived by an experiment in which the change (reduction) of the stress represented by the material is measured with time.

As can be seen in Fig. 4(c), normalized stress-time curve is obtained from stress relaxation test. The Prony series as shown

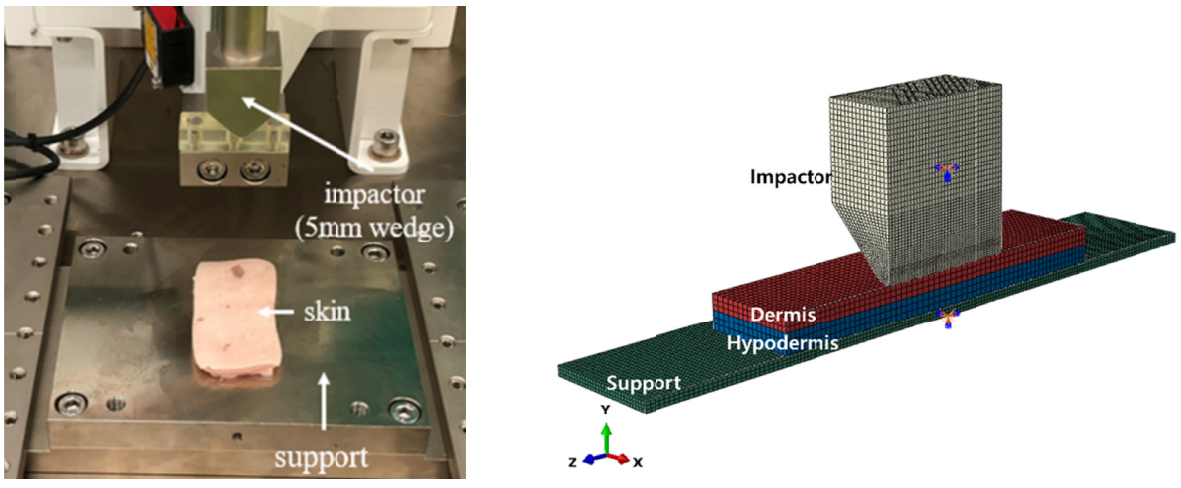

(a) (b)

Fig. 2. (a) Setup for the free-falling test and (b) development of the FEM model

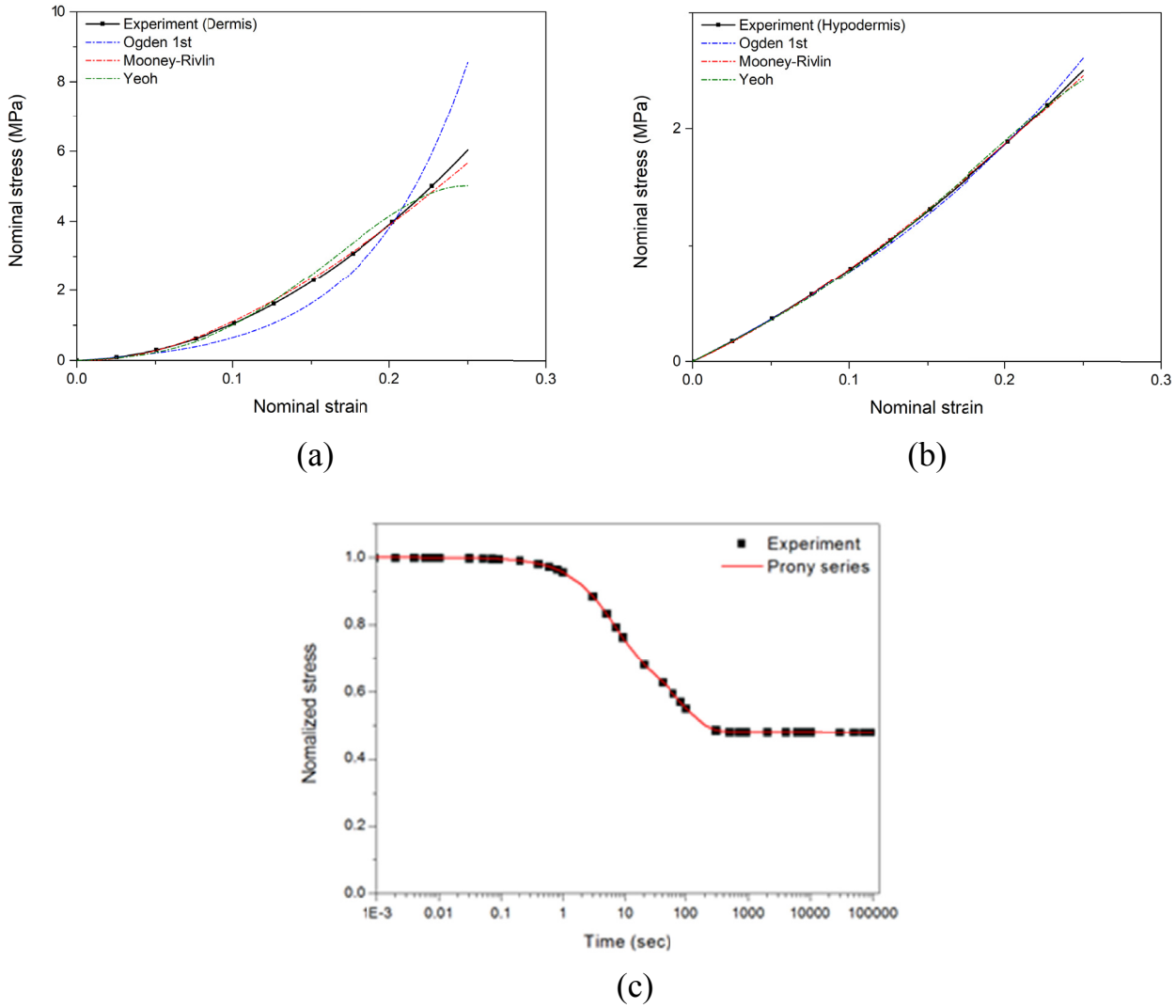

Fig. 3. Fitting of the calibrated hyperelastic models of the (a) dermis and (b) hypodermis. (c) Fitting of the calibrated Prony series model for the stress relaxation data from the uniaxial tension test

in Fig. 3 (c) is expressed using Eq. (2), and the constants are listed in Table 2.

$$G(t) = G_0 - \sum_{i=1}^{N} G_i \left[1 - \exp\left(-t / \tau_i\right)\right] \tag{2}$$

Where G_i is the relaxation modulus, τ_i is the relaxation time. Both are material constant and N is a sum of a series of exponential decays. In order to verify the validity of the mechanical properties of porcine skin after applying the visco-hyperelastic model derived from this study, the FEM model was first implemented as in the experiment (Fig. 2(b)). The analysis process and solver were run in ABAQUS EXPLICIT.

TABLE 2

Calibrated parameters of the Prony series model for the porcine skin

I	G(I)	K(I)	TAU(I)
1	0.567	0	0.986
2	0.163	0	27.773

As can be observed in Fig. 4, the experimental results include the output of the load cell in accordance to the output time of the load cell, while the analyzed results include the contact forces between the impactor and the specimen with reference to Torres et al. [17], respectively.

The maximum impact load and impulse in the falling drop impact test are shown in Fig. 4(a). The error between the experiment and FEM is 15.87% in terms of the maximum impact load, and 19.92% in terms of the impulse corresponding to the maximum force time in Fig. 4(b). As a result, the visco-hyperelastic model of porcine skin does not exactly describe the falling drop impact test result of the porcine skin used in this study, but they are considered to describe the experimental data at a practical level. From the quantified fitting error values, it can be seen that the prediction capability of the constitutive model is not high but moderate. Therefore, the calibrated models can be used only for a rough estimation of the quasi-static mechanical behavior of the porcine skin. Hence, a new strain energy density function is required for an accurate description of the mechanical behavior of the porcine skin with rubber-like behavior.

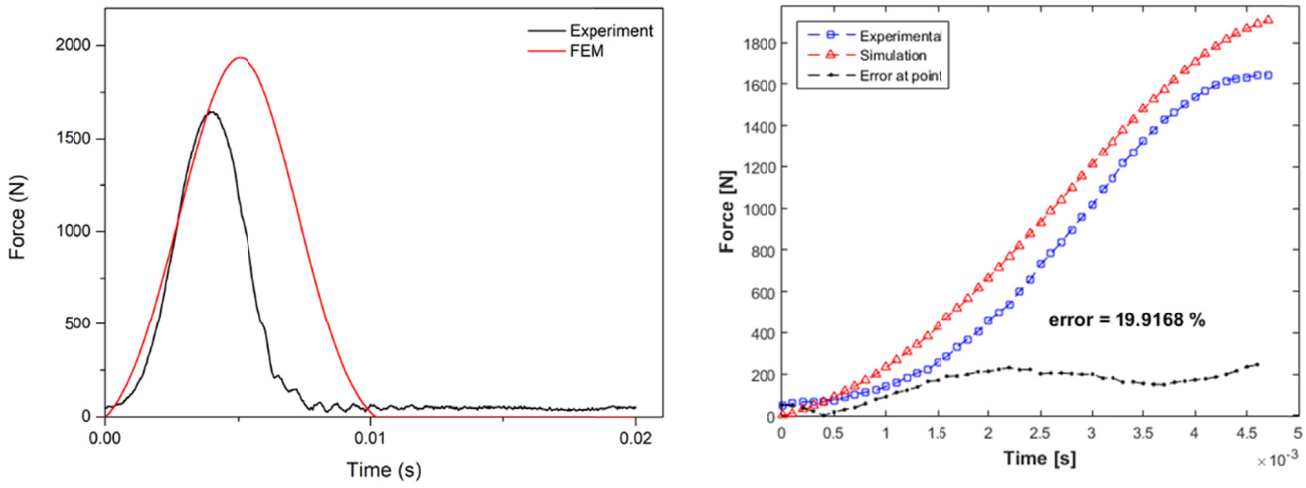

Fig. 4. (a) Comparison of the experimental and FEM force-time responses for the falling drop impact test, and (b) calculated error between the experiment and FEM

4. Conclusions

Based on the quasistatic tensile test, the hyperelastic model was calibrated. The Prony series viscoelastic model was also calibrated using the stress relaxation test. In order to investigate the capability of the calibrated constitutive equation, the free-falling impact tests were carried out. A first-order Ogden and a second-order Prony test models were shown to be appropriate as the best visco-hyperelastic models on porcine skin for the impact test. Even though the calibrated constitutive models cannot describe the free-falling drop test very accurately, they are expected to be of practical use in describing the uniaxial tensile behaviors of porcine skin. In the future, it could be used to predict the injury which would result from the collision between the human and the robot.

Acknowledgments

This research was supported by the Technology Innovation Program (10084657) funded By the Ministry of Trade, Industry & Energy (MOTIE, Korea). It was also financially supported by the Basic Science Research Program under contract numbers 2017R1A6A3A11028683 (S. Kim) funded by the Ministry of Education (Korea).

REFERENCES

[1] C.A. Cordero, G. Carbone, M. Ceccarelli, J. Echávarri, J.L. Muñoz, Mech. Mach. Theory **80**, 184-199 (2014).

[2] J.A. Marvel, J. Falco, I. Marstio, IEEE Trans. Syst. Man Cybern. -Syst. **45** (2), 260-275 (2015).

[3] A.M. Zanchettin, N.M. Ceriani, P. Rocco, H. Ding, B. Matthias, IEEE Trans. Autom. Sci. Eng. **13** (2), 882-893 (2016).

[4] X. Chen, J. Yi, J. Li, J. Zhou, Z. Wang, IEEE Robotics and Automation Letters. **3** (4), 3505-3512 (2018).

[5] J. Lim, J. Hong, W.W. Chen, T. Weerasooriya, Int. J. Impact Eng. **38** (2-3), 130-135 (2011).

[6] G. Uzer, A. Ho, R. Clark, C. Fu-pen, in Proceedings of the Society for Experimental Mechanics Annual Conference (2009).

[7] M. Żak, P. Kuropka, M. Kobielarz, A. Dudek, K. Kaleta-Kuratewicz, S. Szotek, Acta. Bioeng. Biomech. **13** (2), 37-43 (2011).

[8] O.A. Shergold, N.A. Fleck, D. Radford, Int. J. Impact Eng. **32** (9), 1384-1402 (2006).

[9] A. Kalra, A. Lowe, A. Al-Jumaily, J. Mater. Sci. Eng. **5** (4), 254-260 (2016).

[10] J.M. Benítez, F.J. Montáns, Comput. Struct. **190**, 75-107 (2017).

[11] H. Joodaki, M.B. Panzer, Proc. Inst. Mech. Eng. Part H J. Eng. Med. **232** (4), 323-343 (2018).

[12] J.W. Jor, M.P. Nash, P.M. Nielsen, P.J. Hunter, Biomech. Model. Mechanobiol. **10** (5), 767-778 (2011).

[13] J.W. Jor, M.D. Parker, A.J. Taberner, M.P. Nash, P.M. Nielsen, Wiley Interdisciplinary Reviews: Systems Biology and Medicine **5** (5), 539-556 (2013).

[14] W. Li, Biomedical Engineering Letters **5** (4), 241-250 (2015).

[15] D. Remache, M. Caliez, M. Gratton, S. Dos Santos, J. Mech. Behav. Biomed. **77**, 242-249 (2018).

[16] Z. Liu, K. Yeung, J. Mech. Behav. Biomed. Mater. **2** (1), 22-28 (2008).

[17] J.P. Torres, P M. Frontini, L. Aretxabaleta, Polym. Int. **62** (11), 1553-1559 (2013).